

## The $\Lambda(1405)$ with one pole

Eberhard Klempt<sup>1,\*</sup>

<sup>1</sup>HISKP, University of Bonn, Nussallee 14-16, 53115 Bonn

**Abstract.** The  $\Lambda(1405)1/2^-$  resonance is discussed and a fit of the Bonn-Gatchina (BnGa) partial-wave-analysis group is presented to data relevant for this resonance. In the  $\Sigma\pi - N\bar{K}$  coupled channel system, no  $\Sigma$  pole and only one  $\Lambda$  pole in the mass range from the  $\Sigma\pi$  threshold to 1500 MeV is required to get a good description of the data.

### 1 Origin of resonances in strong interactions

The strong interactions support a large variety of bound states and resonances. Different ranges of the interactions lead to different types of states. The  $J/\psi$  meson is a prototype of  $c\bar{c}$  state bound in a Cornell-type potential. In contrast, the  $\chi_{c1}(3872)$  has at least a strong  $D^{*0}\bar{D}^0$  molecular component bound by pion exchange. For some resonances, the interpretation is controversial: the  $N(1535)1/2^-$  is predicted in quark models as  $qqq$  resonance but it can as well be understood as a  $\Lambda\bar{K}-\Sigma\bar{K}$  molecule.

Here, we study the pole content of  $\Sigma\pi$  and  $N\bar{K}$   $S$ -wave interactions in the mass region below 1.5 GeV. In the quark model, one SU(3) singlet resonance is expected which is identified with  $\Lambda(1405)1/2^-$  called  $\Lambda(1405)$  here. However, in the chiral unitary approach, two negative-parity  $\Lambda$  resonances and one or two  $\Sigma$  resonances are found.

\*e-mail: Klempt@hiskp.uni-bonn.de

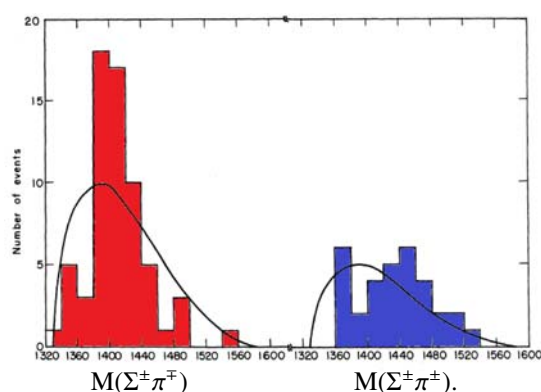


**Figure 1.** (color online) The neutral and like-sign  $M(\Sigma\pi)$  invariant mass distributions from the reactions  $K^-p \rightarrow \Sigma^+\pi^-\pi^+\pi^+$  and  $K^-p \rightarrow \Sigma^-\pi^+\pi^-\pi^-$  [1].

### 2 History

In 1961, the Nobel-prize winner Luis Alvarez and his group [1] analyzed bubble chamber data on the reactions  $K^-p \rightarrow \Sigma^+\pi^-\pi^+\pi^+$  and  $K^-p \rightarrow \Sigma^-\pi^+\pi^-\pi^-$ . The neutral  $M_{\Sigma^+\pi^+}$  invariant mass distribution (with two entries per event) show a clear peak at about 1400 MeV which is absent in the like sign  $M_{\Sigma^-\pi^-}$  invariant mass distribution (see Fig. 1). The  $\Lambda(1405)$  was discovered! A few years later, a measurement has been made of the relative signs of the resonant  $K^-p \rightarrow Y^* \rightarrow \Sigma\pi$  reaction amplitudes with  $Y^* = \Sigma(1385)$ ,  $\Lambda(1405)$ , or  $\Lambda(1520)$ . It was shown that  $\Lambda(1405)$  and  $\Lambda(1520)$  are to be described as predominantly SU(3) singlets [2].

In 1966, Richard H. Dalitz and collaborators showed that the large  $K^-p$  scattering leads to a virtual bound state at 1410 MeV [3]. Since then, the  $\Lambda(1405)$  is *the* paradigm for a dynamically generated state.

In 1995, Kaiser, Siegel and Weise used a chiral Lagrangian to construct a potential for  $S$ -wave meson-baryon scattering [4]. The approach reproduced well the properties of  $\Lambda(1405)$ .

So far, there is not necessarily a conflict between the interpretation of  $\Lambda(1405)$  as  $qqq$  resonance or as dynamically generated  $K^-p$  bound state. Like  $N(1535)1/2^-$ ,  $\Lambda(1405)$  can be both. It could have, e.g., a  $qqq$  core coupling strongly to  $\bar{K}N$  and  $\Sigma\pi$  and developing a mesonic cloud with a three-quark core.

In 2000, this compatibility ceased to be valid when Oller and Meißner studied the  $S$  wave kaonnucleon interactions exploiting an Effective Field Theory (EFT) [5]. Dispersion relations were used to perform the necessary resummation of the lowest order relativistic chiral Lagrangian. They found that the low-mass region houses three negative-parity resonances, one SU(3) singlet and one SU(3) octet  $\Lambda$  and one  $\Sigma$  resonance. The spectrum was interpreted in [6], the interpretation is shown in Fig. 2. The spectrum originates from the interactions of octet baryons and octet mesons. The findings of Refs. [5, 6] have been substantiated by better calculations and various groups over the years, see. [7].

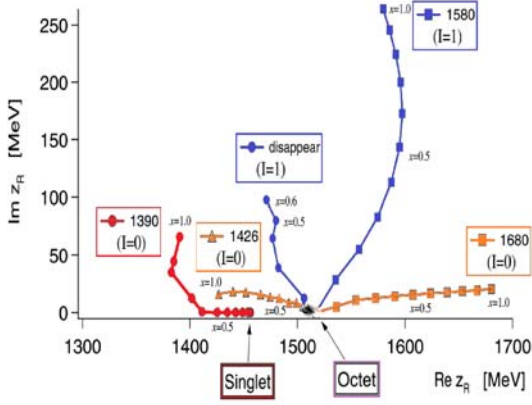


**Figure 2.** (color online) The  $\bar{K}N-\Sigma\pi$  coupled-channel dynamics leads to two pairs of  $\Lambda$  and  $\Sigma$  SU(3) octets and one  $\Lambda$  SU(3) singlet [6].

The three  $\Lambda^*$  poles in Fig. 2 are combinations of the singlet state (at about 1390 MeV) and the two octet states (at about 1426 and 1680 MeV). The isovector states were found to be sensitive on the details of the coupled channel approach. The findings were confirmed in a number of further studies. They were reviewed by Maxim Mai at this conference.

In this contribution, I present an analysis of the BnGa group who fit the most relevant data on the  $\Sigma\pi - \bar{K}N$  coupled channel system [8] and showed that just one resonance,  $\Lambda(1405)$ , is required to get a reasonable description of the data.

### 3 Bonn-Gatchina analysis

#### 3.1 Bonn-Gatchina analysis

In the analysis, we use a modified  $K$ -matrix approach. Instead of the  $K$ -matrix

$$\hat{A} = \hat{K} (I - i\hat{\rho}\hat{K})^{-1}$$

we use

$$A = K (I - Re B\hat{K} - i\hat{\rho}\hat{K})^{-1} \quad \text{with}$$

$$\int \frac{ds'}{\pi} \frac{A_{aj}(s, s')}{s' - s - i\epsilon} \rho_j(s') K_{jb}(s', s) A_{aj}(s, s) \times \\ Re B(s) K_{jb}(s, s) + i A_{aj}(s, s) \rho_j(s) K_{jb}(s)$$

$$\text{where} \quad Re B(s) = \oint \frac{ds'}{\pi} \frac{\rho_j(s')}{s' - s}.$$

Here,  $\oint$  is the principle-value integral. This approach provides a correct continuation of the amplitude below thresholds.

#### 3.2 Data used

We use the CLAS data on the three charge states  $\gamma p \rightarrow K^+(\Sigma^\pm\pi^\mp)$  [9] and Crystal Ball (BNL) data on  $K^-p \rightarrow \pi^0\pi^0\Lambda$  and  $K^-p \rightarrow \pi^0\pi^0\Sigma^0$  at Kaon momenta in the 514 MeV/c to 750 MeV/c MeV momentum range [10]. A subset of the data is shown in Figs. 3 and 4. These two data sets [9, 10] were fitted event-by-event with a maximum likelihood fit. The data on  $\gamma p \rightarrow K^+(\Sigma^0\pi^0)$  [9], shown in Fig. 3(right), were not included in the fit: these data were predicted demonstrating that  $\Lambda(1405)$  and  $\Sigma(1385)$  – which both contribute to the data shown in Fig. 3(left) and Fig. 3(center) – are well identified in the fit. Further included are bubble chamber data on  $K^-p \rightarrow \pi^-\pi^+\pi^+\Sigma^\mp$  [11] (see Fig. 4, right), the differential cross sections for  $K^-p \rightarrow K^-p$  and  $K^0n$  from [12] in the 1464 and 1548 MeV mass range (see Fig. 5, and total cross sections for  $K^-p \rightarrow K^-p, K^0n, \Sigma^+\pi^-, \Sigma^0\pi^0, \Sigma^-\pi^+, \Lambda\pi^0$  [13–16] (see Fig. 6). The fit is constrained by data on the  $K^-p$  system at rest: by the ratios of  $K^-p$  capture rates  $\gamma = \Gamma_{K^-p \rightarrow \pi^+\Sigma^-} / \Gamma_{K^-p \rightarrow \pi^-\Sigma^+}$ ,  $R_n = \Gamma_{K^-p \rightarrow \pi^0\Lambda} / \Gamma_{K^-p \rightarrow \text{neutral}}$ , and  $R_c = \Gamma_{K^-p \rightarrow \pi^+\Sigma^\pm} / \Gamma_{K^-p \rightarrow \text{inelastic}}$  [17, 18], and the recent experimental results on the energy shift and width of kaonic hydrogen atoms  $\Delta E - i\Gamma/2$  which constrain the  $K^-p$   $S$ -wave scattering length [19, 20]. The experimental values are compared to our fit results in Table 1.

**Table 1.** Experimental results for the quantities listed in Eqs. (1) and the fit result.

	Data	Fit
$\Delta E - i\Gamma/2$	$283 \pm 42 - i(271 \pm 55)$	$310 \pm 15 - i(332 \pm 15)$ eV
$\gamma$	$2.38 \pm 0.04$	$2.40 \pm 0.02$
$R_n$	$0.189 \pm 0.015$	$0.209 \pm 0.008$
$R_c$	$0.664 \pm 0.011$	$0.671 \pm 0.010$

Our fit to the elastic differential and the total cross sections is significantly lower than the data. This is a compromise with the data on the strong-interaction width  $\Gamma$  of the  $K^-p$  atom: if the elastic cross section is larger, the width increases as well. Fits based on the chiral unitary approach do better here even though at the expense of a larger number of parameters.

#### 3.3 Parameters

Most relevant here are the  $K^-p - \Sigma\pi$  isoscalar and isovector  $S$ -wave scattering amplitudes. The amplitudes are described by five-channel amplitudes with decays to  $\Sigma^+\pi^-$ ,  $\Sigma^0\pi^0$ ,  $\Sigma^-\pi^+$ ,  $pK^-$  and  $nK^0$ . The mass differences between the three  $\Sigma\pi$  and the two  $N\bar{K}$  channels are taken into account, the relative couplings are fixed by Clebsch-Gordan coefficients. For the isoscalar amplitude, we use a one-pole parameterization. It depends on two real coupling constants ( $g_{\Sigma\pi}$  and  $g_{KN}$ ) and a bare mass value  $M$ . These parameters are defined in the fit. For the isovector channel, we use a two-pole amplitude. Each pole is characterized by the bare mass and three real coupling constants for decays into  $\Sigma\pi$ ,  $N\bar{K}$  and  $\Lambda\pi$ . Thus, this channel needs 8

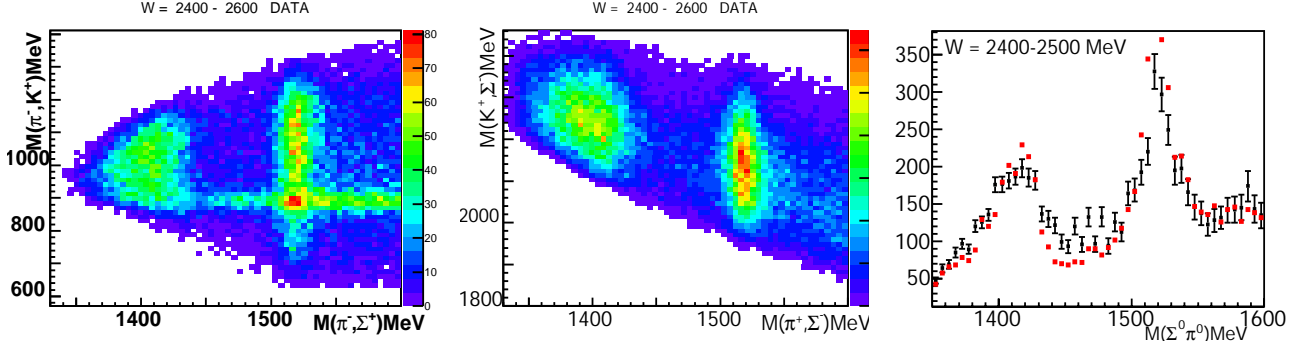


**Figure 3.** (color online)  $\gamma p \rightarrow K^+ \pi^+ \Sigma^\pm$  and for  $2400 < W = M_{\gamma p} < 2600, \text{MeV}$ :  $M(\pi^- K^+)$  versus  $M(\pi^- \Sigma^+)$  (left) and  $M(K^+ \Sigma^-)$  versus  $M(\pi^+ \Sigma^-)$  (center) two-dimensional mass distributions for reconstructed data without acceptance correction. These data were fitted event-by-event in a likelihood fit. Right:  $\Sigma^0 \pi^0$  invariant mass distribution for  $\gamma p \rightarrow K^+ (\Sigma^0 \pi^0)$  and for  $2400 < W = M_{\gamma p} < 2500, \text{MeV}$ . The data are not included in the fit, the points without errors are predictions.

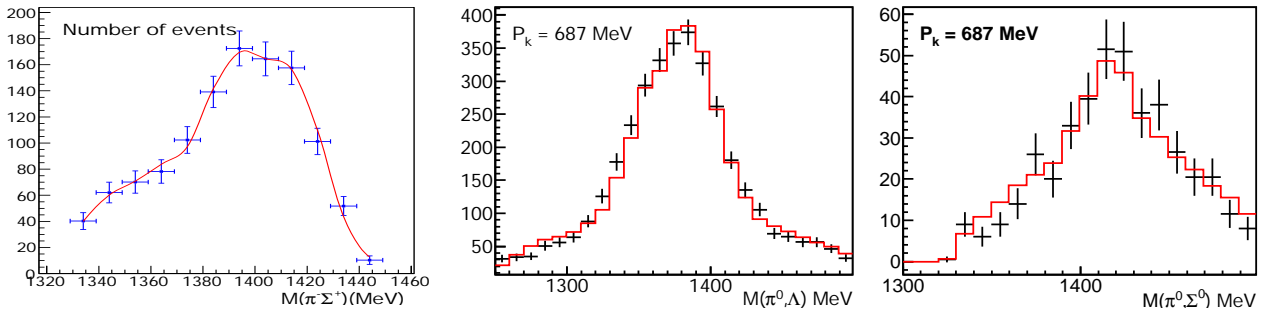


**Figure 4.** (color online) Left:  $\Sigma^+ \pi^-$  mass projection from the reaction  $K^- p \rightarrow \pi^- \pi^+ \pi^+ \Sigma^\pm$  for events with  $M_{\pi^+ \pi^+ \Sigma^\pm}$  compatible with  $\Sigma(1670)3/2^-$  [11]. The Crystal Ball data on  $K^- p \rightarrow \pi^0 \pi^0 \Lambda$  (left) and  $K^- p \rightarrow \pi^0 \pi^0 \Sigma^0$  (right) [10].

parameters. Thus we have 11 parameters to describe the isoscalar and the isovector  $S$ -wave scattering amplitudes. For the fit to elastic scattering and charge exchange, we allow for a small  $P$ -wave contribution. The  $P$ -wave is described by two subthreshold vector poles – one isoscalar, one isovector pole – with two coupling constants.

The production mechanism of the reaction  $\gamma p \rightarrow K^+ \Sigma \pi$  is not known. We describe the initial state by two Breit-Wigner amplitudes in each partial wave for  $J^P = 1/2^\pm, 3/2^\pm, 5/2^\pm$ , and  $7/2^\pm$  (8 resonances with 14 helicity amplitudes) and  $2 \times 4 + 6 \times 8$  free coupling constants for their decays into  $\Sigma(1385)\pi$ ,  $\Lambda(1405)\pi$ ,  $\Lambda(1520)\pi$ , or  $NK^*$ . Thus 78 resonances govern the photoproduction dynamics. The properties of  $\Sigma(1385)$ ,  $\Lambda(1405)$ ,  $\Lambda(1520)$ , and  $K^*$  are taken from the RPP [21].

The bubble chamber data on  $K^- p \rightarrow \pi^- \pi^+ \pi^+ \Sigma^\pm$  [11] are fitted with the assumption that the  $\Lambda(1405)$  stems from  $\Sigma^+(1670)3/2^-$  hyperons decaying in a cascade to  $\Lambda(1405)\pi^+ \rightarrow (\Sigma^\mp \pi^\pm)\pi^+$ . Parameters are the  $\Sigma(1670)3/2^-$  production strength and decay probability. Contributions from  $\Sigma^0(1385) \rightarrow \Sigma^\mp \pi^\pm$  with a  $\approx 25\%$  fraction improve the fit.

## 4 Results

For the low-mass isovector  $S$ -wave, we use two  $K$ -matrix poles. One pole is found far below the  $\Sigma\pi$  threshold; we assume the pole describes the effects of left-hand cuts. One

pole is above the fitted region; we assign it to the lowest-mass  $\Sigma(1620)1/2^-$  resonance. The low-mass isoscalar  $S$ -wave is described by one pole at about 1400 MeV. If we introduce a second pole, this pole moves either to a mass below 1 GeV, or a narrow pole with  $\Gamma \approx 1 \text{ MeV}$  evolves with a mass coinciding with the  $N\bar{K}$  threshold. We disregard this solution. Thus we conclude that the low-energy  $\Sigma\pi-N\bar{K}$   $S$ -wave interactions can be described by one isoscalar pole. Its mass and width are determined to

$$M_{\text{pole}} = 1422 \pm 3 \text{ MeV} \quad \Gamma_{\text{pole}} = 42 \pm 6 \text{ MeV}$$

No further pole is required in the fit in the mass range from threshold to 1.5 GeV, neither a second pole in the  $\Lambda$  sector nor any pole in the  $\Sigma$  sector. A pole search in the complex plane identified one pole as well.

## 5 Discussion

In the quark model, the  $\Lambda(1405)$  is a (dominantly)  $SU(3)$  singlet baryon. Experimentally, the singlet nature can be deduced from the sign of the imaginary part of the  $F$  amplitude at the resonance position, see Fig. 99.1 in [21]. In analyses based on EFT's, the narrow state at 1420 MeV is a (dominantly) octet state. This is shown in Fig. 2, and it follows from Figure 7 taken from Ref. [26]. The Figure shows the real and imaginary part of the  $K^- p \rightarrow \Lambda(1405) \rightarrow \Sigma\pi$  transition amplitude. At the  $\Lambda(1405)$  mass,

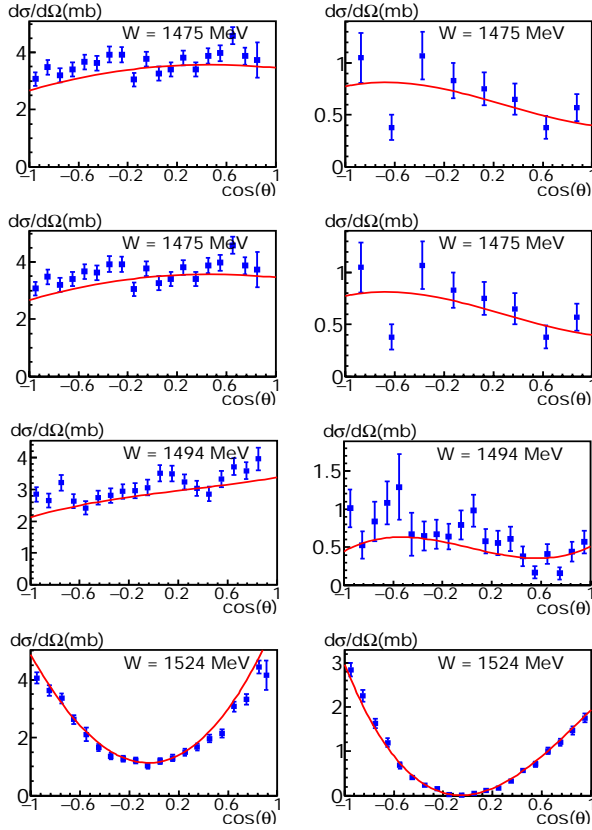


**Figure 5.** Selected differential cross sections for  $K^-p \rightarrow K^-p$  (left) and  $K^-p \rightarrow \bar{K}^0n$  (right) from [12]. Data were taken between 1464 and 1548 MeV invariant mass and reported in 25 bins. Shown are three bins. The fit is given by the line.

the amplitude is proportional to  $-i$ ; this identifies the resonance is a SU(3)-octet resonance. The decisive difference between conventional interpretations of the  $\Lambda(1405)$  and EFT-based analyses is the question: Is the  $\Lambda(1405)$  dominantly a SU(3)-singlet or a SU(3)-octet state?

The  $\Lambda(1405)$  is, of course, not the only  $\Lambda$  excitation. The spectrum of low-mass  $\Lambda$  and  $\Sigma$  resonances is known since long; recently, it has been determined again and many “candidate” states were disregarded, a few new resonances were discovered [22, 23]. The low-mass spectrum is compared to nucleon excitations in Table 2.

The  $\Lambda(1405)$  can be identified as (dominantly) SU(3)-singlet state and as the expected spin partner of  $\Lambda(1520)$ . Its mass is rather low, this is a well-known problem of quark models. It may be noted that a simple mass formula – using the masses of nucleon,  $\Delta$  and  $\Omega$  and the Regge slope as only input variables – predicts 1460 MeV for the two singlet states [24]. In the (dominantly) SU(3) octet, there are the ground states and radial excitations with  $(N, L^P, S) = (2, 0^+, 1/2)$  from the 56 and 70-plet, the negative-parity states  $(N, L^P, S) = (1, 1^-, 1/2)$  and  $(1, 1^-, 3/2)$ , and the positive-parity states with  $(N, L^P, S) = (2, 2^+, 1/2)$ . The  $\Lambda$  and  $\Sigma$  resonances are 100 to 150 MeV above the corresponding nucleon states. A further spin doublet of  $\Sigma$  states with  $J^P = 1/2^-$  is expected (and seen in [22, 23]) that would correspond to the  $\Delta(1620)1/2^-$  and  $\Delta(1700)3/2^-$  doublet. All these states were found, only

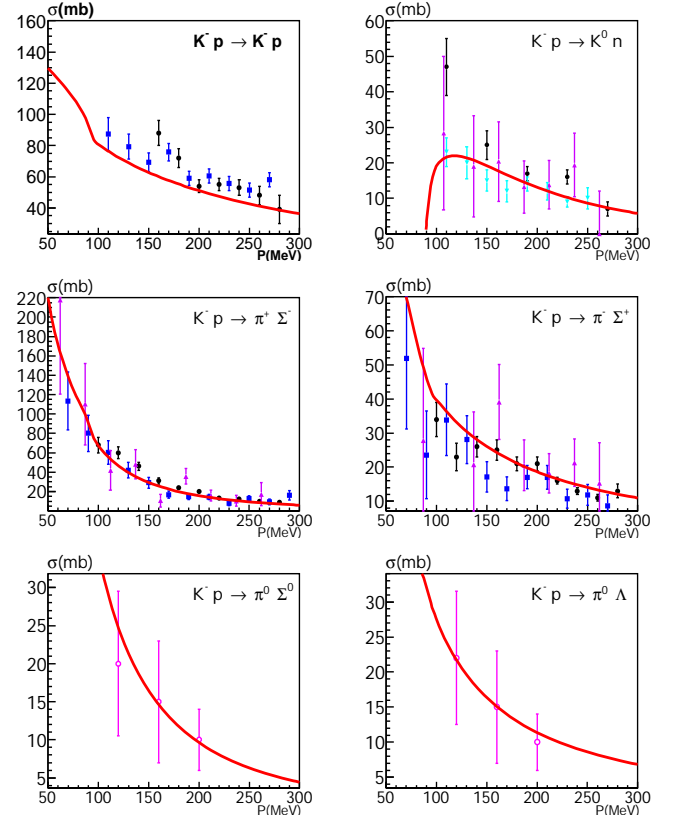


**Figure 6.** The total cross sections for  $K^-p$  induced reactions:  $K^-p \rightarrow K^-p$ ,  $K^-p \rightarrow \bar{K}^0n$ ,  $K^-p \rightarrow \pi^-\Lambda$ ,  $K^-p \rightarrow \pi^-\Sigma^-$ ,  $K^-p \rightarrow \pi^-\Sigma^0$ ,  $K^-p \rightarrow \pi^-\Sigma^+$  [13–16]. The single pole  $\Lambda(1405)$  fit is given as the red curve.

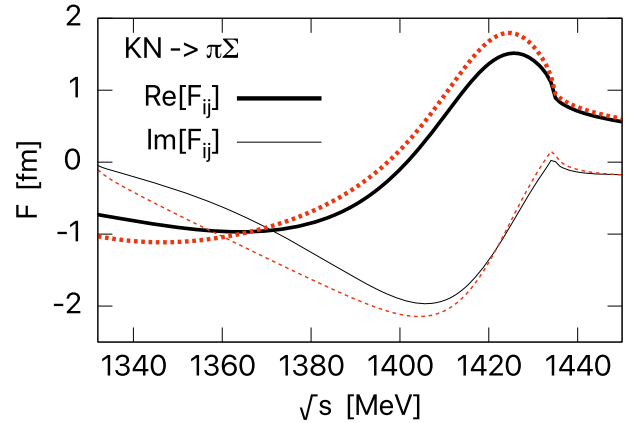


**Figure 7.** Real and imaginary part of the  $K^-p \rightarrow \Lambda(1405) \rightarrow \Sigma\pi$  transition amplitude  $F$  [26]. At  $\text{Re}[F] = 0$ ,  $\text{Im}[F]$  is negative, suggesting that the dominant part of the amplitude at 1410 MeV is a SU(3) octet.

the  $J^P = 3/2^-$  from the spin triplet is again missing. The qualitative agreement – at least in the number and mass ordering of the states – of the observed states with those reported in [25] supports the quark-model interpretation of the hyperon spectrum.

One might think that the quark-model states are what they are, and  $\Lambda(1350)$  comes in addition as a dynamically

generated resonance. But the problem is not the  $\Lambda(1350)$  but the  $\Lambda(1405)$ : in the quark model,  $\Lambda(1405)$  in a SU(3) singlet resonance, in EFT analyses, it is an octet. As octet resonance, it does not fit into the spectrum of  $\Lambda$  resonances. A possible escape would be to assume that all states in Table 3 derived from EFT's are generated in addition to the quark-model states. In this case,  $\Lambda(1405)$  and  $\Lambda(1670)$  should need to have a double-pole structure; with one  $\Lambda(1405)$  being a SU(3) octet, the other one a SU(3) singlet. We remind of the fact that there was the hope to find a double-pole structure for  $N(1535)$  but there has never been any evidence for two close-by  $N(1535)$  poles. For the  $\Lambda(1405)$  we do not find any hint for a double-pole structure.

Can we understand how two low-mass  $\Lambda$  resonances with  $J^P = 1/2^-$  can appear in the analysis? We first assume that  $\Lambda(1405)$  is a SU(3)-singlet state. If the fit forces it to be an octet, the  $K^-p \rightarrow \Lambda(1405) \rightarrow \Sigma\pi$  transition amplitude has the wrong sign; this could be compensated by adding a further SU(3) singlet resonance at about the same mass. Technically, we can thus understand why fits finding  $\Lambda(1405)$  as SU(3) octet state need at least one additional resonance. If we assume, instead, the  $\Lambda(1405)$  to be a SU(3) octet state, there is no reason why it should show up as SU(3) singlet in fits with a single pole. The singlet nature of the  $\Lambda(1405)$  is decisive for the interpretation of the low-lying  $\Lambda$  resonances.

The analyses based on EFT's find two  $\Lambda^*$  resonances with  $J^P = 1/2^-$  in the region below 1500 MeV. Why are there two resonances in those analyses and why do we find only one? The main difference may originate from the different interpretations of resonances and interactions. In chiral perturbation theory, resonances are generated dy-

namically from attractive interactions. In the expansion

$$8 \otimes 8 = 1 \oplus 8_1 \oplus 8_2 \oplus 10 \oplus 27,$$

the same multiplets are expected as in the quark model:

$$3 \otimes 3 \otimes 3 = 1 \oplus 8_1 \oplus 8_2 \oplus 10,$$

except for the 27-plet which is absent in the quark model. The latter plet is supposed not to lead to attractive interactions. Thus in both scenarios, there is one singlet and two octet-states with  $J^P = 1/2^-$ . (In the quark model, this is a simplified view; both octets are combined with spin states to form the total-quark-spin 1/2 and 3/2.) These three expected  $\Lambda$  states, one mainly singlet and two mainly octet states, are assigned to different physical states (Table 3).

In our approach, these three states generate the attractive interactions: Each  $\Lambda$  pole leads to an attractive interaction in the  $\bar{K}N$  and in the  $\Sigma\pi$  channel. In EFT's, there are primarily the interactions; the  $\bar{K}N$  and  $\Sigma\pi$  interactions are attractive and generate the poles. Our result yields a different answer to the chicken-and-egg problem: what is first, the interaction or the pole? In our approach to the  $\Lambda(1405)$ , the pole creates the largest part of the interactions and the pole is not generated by the interaction.

## 6 Outlook

What can be done to identify the SU(3) structure of  $\Lambda(1405)$  unambiguously? This may be achieved by a study of the reaction

$$J/\psi \rightarrow \bar{\Lambda} (\Sigma^\pm \pi^\mp) + c.c.$$

which is seen with a branching ratio of  $(0.83 \pm 0.07) \cdot 10^{-3}$ . The  $J/\psi$  is of course a SU(3) singlet, the  $\Lambda$  a SU(3) octet. Hence the  $\Sigma\pi$  system forms a SU(3) octet. For zero relative orbital angular momentum in the final state, the  $\Sigma\pi$  system must have the quantum numbers  $J^P = 1/2^-$  or  $3/2^-$ . The  $\bar{\Lambda}\Lambda(1405)$ ,  $\bar{\Lambda}\Lambda(1520)$ , and  $\bar{\Lambda}\Lambda(1670)$  final states can be reached only by the SU(3) octet components of the excited  $\Lambda$ . In EFT's, the  $\Lambda(1405)$  is an octet state, hence the branching ratio for  $J/\psi \rightarrow \bar{\Lambda}\Lambda(1405)$  should be much larger than the one for  $J/\psi \rightarrow \bar{\Lambda}\Lambda(1520)$  and larger (due to the larger phase space) than the one for  $J/\psi \rightarrow \bar{\Lambda}\Lambda(1670)$ . In the quark model, only the latter branching ratio should be sizable and the two former branching ratios should be seen with a similar (small) rate.

*I would like to thank the organizers of NSTAR2019 for the kind invitation and A.V. Anisovich, V.A. Nikonov, A.V. Sarantsev, and U. Thoma for a long and fruitful collaboration.*

Note added in proof: After the conference, a second fit was made in which the presence of two  $\Lambda$  resonances with  $J^P = 1/2^-$  was assumed. A fit with free mass and width gave a pole at the  $K^-p$  threshold and a very narrow width. When the width was fixed to 180 MeV, a shallow minimum at a mass of  $1387 \pm 3$  MeV was observed. The description of the data was similar in quality.

**Table 2.** The  $\Lambda$  excitation spectrum in comparison with the  $\Sigma$  and  $N$  excitation spectra. The  $\Lambda(1850)3/2^-$  and  $\Sigma(1760)3/2^-$  are missing, the masses are estimates.

8	$\Lambda(1890)3/2^+$ $\Sigma(1940)3/2^+$ $N(1720)3/2^+$	$\Lambda(1820)5/2^+$ $\Sigma(1915)5/2^+$ $N(1680)5/2^+$
8	$\Lambda(1810)1/2^+$ $\Sigma(1880)1/2^+$ $N(1710)1/2^+$	
8	$\Lambda(1800)1/2^-$ $\Sigma(1750)1/2^-$ $N(1650)1/2^-$	$\Lambda(1850)3/2^-$ $\Sigma(1760)3/2^-$ $N(1700)3/2^-$
1	$\Lambda(1710)1/2^+$	$\Lambda(1830)5/2^-$ $\Sigma(1775)5/2^-$ $N(1675)5/2^-$
8	$\Lambda(1670)1/2^-$ $\Sigma(1620)1/2^-$ $N(1535)1/2^-$	$\Lambda(1690)3/2^-$ $\Sigma(1670)3/2^-$ $N(1520)3/2^-$
8	$\Lambda(1600)1/2^+$ $\Sigma(1660)1/2^+$ $N(1440)1/2^+$	
1	$\Lambda(1405)1/2^-$	$\Lambda(1520)3/2^-$
8	$\Lambda(1116)$ $\Sigma(1193)$ $N(940)$	

## References

- [1] M. H. Alston, L. W. Alvarez, P. Eberhard, M. L. Good, W. Graziano, H. K. Ticho and S. G. Wojcicki, *Phys. Rev. Lett.* **6**, 698 (1961).
- [2] R. D. Tripp, R. O. Bangerter, A. Barbaro-Galtieri and T. S. Mast, *Phys. Rev. Lett.* **21**, 1721 (1968).
- [3] R. H. Dalitz, T. C. Wong and G. Rajasekaran, *Phys. Rev.* **153**, 1617 (1967).
- [4] N. Kaiser, P. B. Siegel and W. Weise, *Nucl. Phys. A* **594**, 325 (1995).
- [5] J. A. Oller and U.-G. Meißner, *Phys. Lett. B* **500**, 263 (2001).
- [6] D. Jido, J. A. Oller, E. Oset, A. Ramos and U.-G. Meißner, *Nucl. Phys. A* **725**, 181 (2003).
- [7] A. Cieply, M. Mai, U.-G. Meißner and J. Smejkal, *Nucl. Phys. A* **954**, 17 (2016).
- [8] A. V. Anisovich, A. V. Sarantsev, V. A. Nikonov, V. Burkert, R. A. Schumacher, U. Thoma and E. Klempt, arXiv:1905.05456 [nucl-ex].
- [9] K. Moriya *et al.* [CLAS Collaboration], *Phys. Rev. C* **87**, 035206 (2013).
- [10] S. Prakhov *et al.* [Crystall Ball Collaboration], *Phys. Rev. C* **70**, 034605 (2004).
- [11] R. J. Hemingway, *Nucl. Phys. B* **253**, 742 (1985).
- [12] T. S. Mast, M. Alston-Garnjost, R. O. Bangerter, A. S. Barbaro-Galtieri, F. T. Solmitz and R. D. Tripp, *Phys. Rev. D* **14**, 13 (1976).
- [13] W. E. Humphrey and R. R. Ross, *Phys. Rev.* **127**, 1305 (1962).
- [14] M. B. Watson, M. Ferro-Luzzi and R. D. Tripp, *Phys. Rev.* **131**, 2248 (1963).
- [15] M. Sakitt, T. B. Day, R. G. Glasser, N. Seeman, J. H. Friedman, W. E. Humphrey and R. R. Ross, *Phys. Rev.* **139**, B719 (1965).
- [16] J. Ciborowski *et al.*, *J. Phys. G* **8**, 13 (1982).
- [17] D. N. Tovee *et al.*, *Nucl. Phys. B* **33**, 493 (1971).
- [18] R. J. Nowak *et al.*, *Nucl. Phys. B* **139**, 61 (1978).
- [19] M. Bazzi *et al.* [SIDDHARTA Collaboration], *Phys. Lett. B* **704**, 113 (2011).
- [20] M. Bazzi *et al.*, *Nucl. Phys. A* **881**, 88 (2012).
- [21] M. Tanabashi *et al.* [Particle Data Group], *Phys. Rev. D* **98**, no. 3, 030001 (2018).
- [22] M. Matveev, A. V. Sarantsev, V. A. Nikonov, A. V. Anisovich, U. Thoma and E. Klempt, arXiv:1907.03645 [nucl-ex], accepted for publication in EPJA.
- [23] A. V. Sarantsev, M. Matveev, V. A. Nikonov, A. V. Anisovich, U. Thoma and E. Klempt, arXiv:1907.13387 [nucl-ex], accepted for publication in EPJA.
- [24] E. Klempt, *Phys. Rev. C* **66**, 058201 (2002).
- [25] U. Löring, B. C. Metsch and H. R. Petry, *Eur. Phys. J. A* **10**, 447 (2001).
- [26] K. Miyahara, T. Hyodo and W. Weise, *Phys. Rev. C* **98**, no. 2, 025201 (2018).

**Table 3.** The three lowest  $\Lambda$  states with  $J^P = 1/2^-$ .

SU(3)	EFT	QM
1	$\Lambda(1350)$	$\Lambda(1405)$
8	$\Lambda(1405)$ $\Sigma(1401)$	$\Lambda(1670)$ $\Sigma(1620)$
8	$\Lambda(1670)$ $\Sigma(1488)$	$\Lambda(1800)$ $\Sigma(1750)$